# CEPC NOTE

July 10, 2018

# Data-taking strategy for precise measurement of $W$ mass with threshold scan at circular electron positron collider


**Abstract**

The future Circular Electron Positron Colliders, such as the CEPC and FCC-ee, are proposed to make precise measurement of the Higgs boson, verify the Standard Model, explore physic beyond the Standard Model and son on. One important task of them is operating at a center-of-mass energy around the $W$-pair threshold to measure the $W$ boson mass with high precison, which is depended on the data taking strategy. In this paper, the Optimization of the data taking scheme is performed. In case of taking data at three energy points, with $\mathcal{L} = 3.2\ \text{ab}^{-1}$, the precison of $\Delta m_W \sim 1.0$ MeV, as well as the precison of 2.8 MeV for $W$ width, can be achieved.

# 1 Introduction

In the Standard Model (SM) of particle physics, the electroweak (EW) interaction is mediated by the $W$ boson, the $Z$ boson, and the photon, in a gauge theory based on the $SU(2)_L \times U(1)_Y$ symmetry [1–3]. The so called symmetry-breaking mechanism, relies on the interaction of the gauge bosons with a scalar doublet field and implies the existence of an additional physical state known as the Higgs boson [4–6]. In 1983, CERN first established the existence of the $W$ and $Z$ [7–10]. The Higgs boson was first discovered by LHC Collaborations ATLAS and CMS in 2012 [11, 12].

In the EW theory, the $W$-boson mass, $m_W$, can be expressed as function of the $Z$-boson mass, $m_Z$, the fine-structure constant, $\alpha$, the Fermi constant, $G_\mu$, the top-quark mass, $m_t$, and the Higgs boson mass, $m_H$. With the measured values of these parameters, the SM prediction of $m_W$ is $m_W = 80.358 \pm 0.008$ GeV in Ref. [13] and $m_W = 80.362 \pm 0.008$ GeV [14]. The current Partical Data Group (PDG) world average value of $m_W = 80.385 \pm 0.015$ MeV [15] is dominated by the LEP2 and Tevatron, and the latest measurement of $m_W$ is presented by ATLAS at $\sqrt{s} = 7$ TeV, with the result $m_W = 80.370 \pm 0.019$ MeV. In the context of global fits to the SM parameters, constraints on physics beyond the SM are currently limited precision of the $W$-boson mass measurement. The high precision measurement of $m_W$ is very essential to test the overall consistency of the SM and search the physics beyond the SM.

The current results of $m_W$ are almost measured with the direct reconstruction method, with the final states from $W$ decays. This method suffers the large systematic uncertainty, *e.g.*, the uncertainties associated with the modeling of hadronization, the radiative corrections, the energy scale of lepton, and the missing energy. Alternatively, a precise direct determination of the $W$ mass can be achieved by comparing the observed $W$-pair production cross section near its kinematic threshold, and the one calculated with the EW theory. This method is available because the production cross section of $W$-pair is very sensitive to the mass and width of $W$ boson near the $W$-pair threshold, and it only involves counting events, which is clean and uses all decay channels. The advantage of this method is that it is only sensitive to the number of events, *i.e.*, the statistics of data, and the precision of the $W$-pair production cross section.

In this study, the possibility of extracting the $W$ mass, as well as its width, is explored, with the total integrated luminosity of data assumed as $\mathcal{L} = 3.2$ ab$^{-1}$. Because the data taking scheme, includes the number of data taking points, the energy of each data point, and the allocation of the integrated luminosity, is depend on the statistical and systematic uncertainties of $m_W$ and $\Gamma_W$, the study of the uncertainty is performed firstly, which is described in section 2. Then different data taking schemes are investigated in section 3.

# 2 Theoretical tool and uncertainty analysis

In this study, the GENTLE version 2.0 [16] program is used to calculate $\sigma_{WW}$ as a function of the energy ($E_{CM}$), W mass ($m_W$) and width ($\Gamma_W$). Figure 1 shows the cross sections of $W$-pair as a function of the center-of-mass (c.m.) energy with $m_W$ and $\Gamma_W$ fixed to the PDG [15] average values $m_W = 80.385$ GeV and $\Gamma_W = 2.085$ GeV, with the on-shell (off-shell) Born level, as well as the off-shell level with Initial State Radiative (ISR) correction.

## 2.1 Statistical uncertainty

The observed $W$-pair cross section of a specific energy point is:

$$\sigma_{\mathrm{WW}} = \frac{N_{WW}}{\mathcal{L}\epsilon} = \frac{N_{\mathrm{obs}} - N_{\mathrm{B}}}{\mathcal{L}\epsilon}, \tag{1}$$

where $N_{WW}$ is the signal yields; $N_{\mathrm{obs}}$ and $N_{\mathrm{B}}$ are the number of observed and background events, respectively; $\mathcal{L}$ is the integrated luminosity; and $\epsilon$ is the event selection efficiency of signal events.

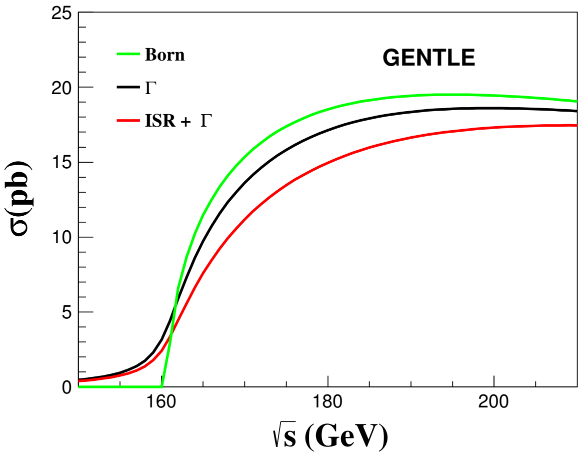


Figure 1: The cross sections of $W$-pair as a function of the c.m. energy of the $e^+e^-$ collision, with the $m_W$ and $\Gamma_W$ fixed to the PDF average values. The green curve is the Born cross section with zero-width assumption, the black one is the Born cross section with the off-shell correction (the $W$ width is taken into account), and the red one is cross section with the off-shell and ISR corrections.

So the statistical uncertainty of the $\sigma_{\text{obs}}$ can be written as (Poisson distribution):

$$\Delta\sigma_{\text{obs}}(\text{stat.}) = \frac{\sqrt{N_{\text{obs}}}}{\mathcal{L}\epsilon} = \frac{\sqrt{\sigma_{\text{obs}}}}{\sqrt{\mathcal{L}\epsilon P}}, \quad \text{P} = \frac{\epsilon\sigma_{\text{WW}}}{\epsilon\sigma_{\text{WW}} + \epsilon_{\text{B}}\sigma_{\text{B}}} \tag{2}$$

where $P$ is the purity of signal events, $\epsilon_B$ is the event selection efficiency of background events.

When taking data at single energy point, the statistical sensitivity to the $W$ mass or width is:

$$\begin{aligned} \Delta m_W(\text{stat.}) &= (\frac{\partial\sigma_{\text{obs}}}{\partial \text{m}_\text{W}})^{-1} \times \Delta\sigma_{\text{obs}} = (\frac{\partial\sigma_{\text{obs}}}{\partial \text{m}_\text{W}})^{-1} \times \frac{\sqrt{\sigma_{\text{obs}}}}{\sqrt{\mathcal{L}\epsilon P}}, \\ \Delta\Gamma_W(\text{stat.}) &= (\frac{\partial\sigma_{\text{obs}}}{\partial\Gamma_\text{W}})^{-1} \times \Delta\sigma_{\text{obs}} = (\frac{\partial\sigma_{\text{obs}}}{\partial\Gamma_\text{W}})^{-1} \times \frac{\sqrt{\sigma_{\text{obs}}}}{\sqrt{\mathcal{L}\epsilon P}}. \end{aligned} \tag{3}$$

Figure 2 shows the statistical uncertainty of $m_W$ and $\Gamma_W$ as a function of the c.m. energy. When taking data at the lowest point of Fig. 2 (a) or (b), the minimal statistical uncertainty of $m_W$ or $\Gamma_W$ can be obtained, but only one of them can be determined with one data point.

When there are more than one data points, the $m_W$ and $\Gamma_W$ can be measured simultaneously. The statistical uncertainties can be obtained by the covariance matrix, which is the inverse of the second derivative matrix of the (log-likelihood or $\chi^2$) function with respect to its free parameters, usually assumed to be evaluated at the best values (the function minimum). The minimum $\chi^2$ method is used in this study and the $\chi^2$ can be constructed as Eq. 4, which is minimized by MINUIT.

$$\chi^2 = \sum_i \frac{(N_{\text{fit}^i} - N^i_{\text{obs}})^2}{N^i_{\text{obs}}} = \frac{(\mathcal{L}\epsilon P)^i(\sigma^i_{\text{fit}} - \sigma^i_{\text{obs}})^2}{\sigma^i_{\text{obs}}}. \tag{4}$$

So, the covariance matrix can be written as:

$$V = \frac{1}{2} \times \begin{pmatrix} \frac{\partial^2\chi 2}{\partial m^2_W} & \frac{\partial^2\chi 2}{\partial m_W \partial\Gamma_W} \\ \frac{\partial^2\chi 2}{\partial m_W \partial\Gamma_W} & \frac{\partial^2\chi 2}{\partial m^2_{\Gamma_W}} \end{pmatrix}^{-1} = \sum_i \begin{pmatrix} \frac{(\mathcal{L}\epsilon P)^i}{\sigma^i_{\text{obs}}}(\frac{\partial\sigma}{\partial m_W})^2 & \frac{(\mathcal{L}\epsilon P)^i}{\sigma^i_{\text{obs}}}\frac{\partial\sigma}{\partial m_W}\frac{\partial\sigma}{\partial\Gamma_W} \\ \frac{(\mathcal{L}\epsilon P)^i}{\sigma^i_{\text{obs}}}\frac{\partial\sigma}{\partial m_W}\frac{\partial\sigma}{\partial\Gamma_W} & \frac{(\mathcal{L}\epsilon P)^i}{\sigma^i_{\text{obs}}}(\frac{\partial\sigma}{\partial m_W})^2 \end{pmatrix}^{-1}. \tag{5}$$

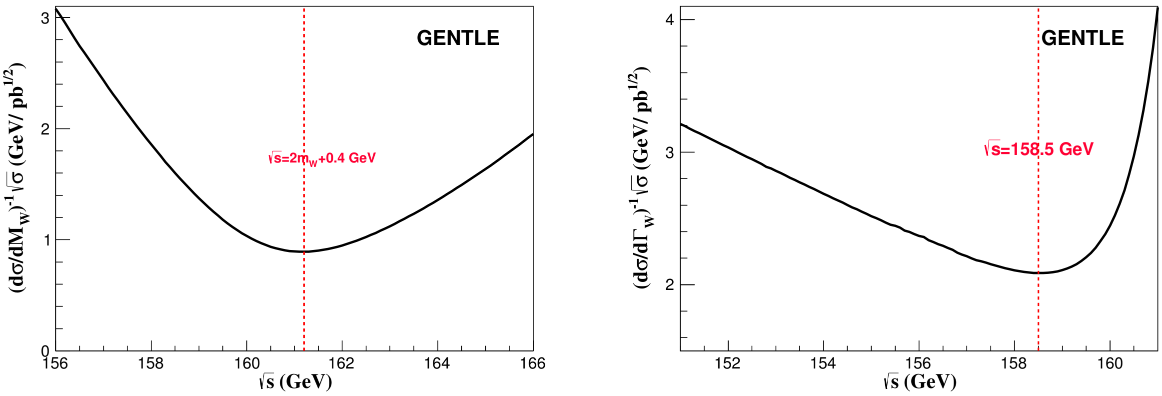


(a) (b)

Figure 2: The statistical uncertainties of $m_W$ and $\Gamma_W$ when taking data at a single energy point.

The diagonal elements of the second derivative matrix, are de-coupled from the other parameter(s), but when the matrix is inverted, the diagonal elements of the inverse contain contributions from all the elements of the second derivative matrix, which is the correlations come from. When the number of fit parameters reduce to one, the Eq. 5 will be simplified to Eq. 3.

## 2.2 Systematic uncertainties

Since the $m_W$ ($\Gamma_W$) is obtained by fit the observed cross section of $W$-pair, $\sigma_{WW}$, with the theoretical calculated cross section, the systematic uncertainties mainly originate from the calculation of $\sigma_{WW}$, the integrated luminosity, the detection efficiency, the purity, the beam energy and its spread, and so on.

If there are more than one data taking points, the systematic uncertainties described above can be divided into two categories:

- Uncorrelated uncertainty: This category includes the uncertainties associated with the beam energy calibration, $\Delta E$; and beam energy spread, $\Delta E_{\mathrm{BS}}$.
- Correlated uncertainty: This category includes the uncertainties from the integrated luminosity, $\Delta\mathcal{L}$; the detection efficiency, $\Delta\epsilon$; the purity, $\Delta P$; and the theoretical $W$-pair cross section, $\Delta\sigma_{\mathrm{th}}$. Generally, this type of uncertainties contains some common trends at different energy points, which can be taken into account in the further analysis.

### 2.2.1 The uncorrelated uncertainties

The uncorrelated uncertainties, $\Delta E$ and $\Delta E_{BS}$, are dominantly based on the collider performance during the data taking. With the beam energy spread, the observed cross section of a specific energy point can be written as:

$$\begin{aligned}\sigma_{\mathrm{obs}}(E_0) &= \int_0^{\infty} \sigma(E^{'}) \times G(E_0, E_{BS}) dE^{'} \\ &= \int_0^{\infty} \sigma(E^{'}) \times \frac{1}{2\sqrt{\pi}E_{BS}^{0}} e^{\frac{-(E_0-E^{'})^2}{4E_{BS}^{02}}} dE^{'},\end{aligned} \tag{6}$$

where $E_0$ is the calibrated energy of the data point, $E_{BS}^0$ is the nominal beam energy spread, and $E^{'}$ is the true energy, which follows Gaussian distribution. We assume that there is no correlation between the two beams, so the total uncertainty associated with beam energy spread is $\sqrt{2}E_{BS}$.

With the $\Delta E$ and $\Delta E_{BS}$, the $\sigma_{\text{obs}}$ becomes:

$$\sigma_{\text{obs}}(E_0) = \int_0^{\infty} \sigma_{\text{TH}}(E^{'}) \times \frac{1}{2\sqrt{\pi}E_{BS}} e^{\frac{-(E-E^{'})^2}{4E_{BS}^2}} dE^{'}, \tag{7}$$

where $E$ is the energy with its uncertainty, $E = G(E_0, \sqrt{2}\Delta E)$, and $E_{BS}$ is the energy spread with its uncertainty, $E_{BS} = G(E_{BS}^0, \sqrt{2}\Delta E_{BS})$. Figure 3 (a) shows the dependence of uncertainty of $W$ mass, $\Delta m_W$, on the $\Delta E$, with a fixed energy. We can see that the $\Delta m_W$ is almost increase linearly with the $\Delta E$. When the $\Delta E$ is fixed, the $\Delta m_W$ is near insensitive to the energy, which is shown in Fig. 3 (b). The distributions of $W$-pair cross section with different beam energy spreads are shown in Fig 4, where the Y-axis is the ratio between the cross sections with different $E_{BS}$ and the one without $E_{BS}$. It can be noted that the dependence of cross section on the beam energy spread intersects at a point, with $E \approx 2m_W + 1.3$ GeV, where the cross section is insensitive to the beam energy spread.

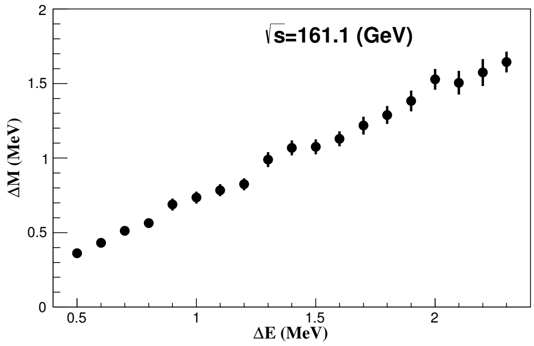


(a)

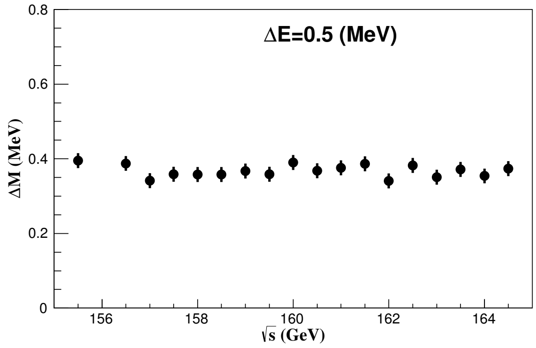


(b)

Figure 3: (a)The dependence of uncertainty of $W$ mass , $\Delta m_W$, on the $\Delta E$, with a fixed energy. (b)The dependence of $\Delta m_W$ on the energy, with a fixed $\Delta E$.

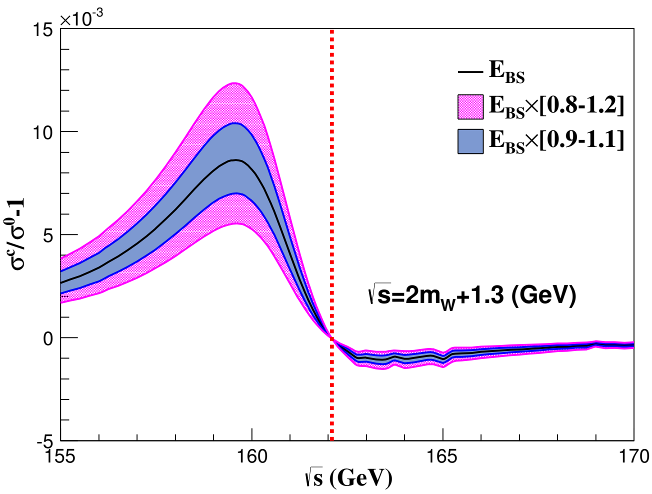


Figure 4: The distribution of the ratio between the cross sections with different $E_{BS}$ and the one without $E_{BS}$. The central curve corresponds to the prediction obtained with $E_{BS} = 0.16\%$ (relative value), which is the design value of CEPC. Purple and blue bands show the ratio curves obtained varying the $E_{BS}$.

### 2.2.2 The correlated uncertainties

With the contributions from the correlated uncertainties, which include the $\Delta\mathcal{L}$, $\Delta\epsilon$, $\Delta P$, and $\Delta\sigma_{th}$, the observed numbers of $W$-pair events at different data points become large or small at the same time, which is the meaning of the correlation.

Since $N_{\text{obs}} = \mathcal{L}\sigma_{\text{th}}\epsilon P$, these correlated uncertainties described above, will contribute to the $\Delta m_W$ ($\Delta\Gamma_W$) in same way. So we just take the $\Delta\mathcal{L}$ as an example. With uncertainty, the luminosity of a specific data point is in the form:

$$\mathcal{L} = G(\mathcal{L}_0, \mathcal{L}_0 \cdot \sigma_{\mathcal{L}}), \tag{8}$$

where $\mathcal{L}_0$ is the nominal value and $\sigma_{\mathcal{L}}$ is the relative uncertainty of $\mathcal{L}_0$, which is keep same value among different data points. To consider the $\Delta m_W$ associated with $\Delta\mathcal{L}$, the nominal luminosity, $\mathcal{L}_0$ is used in the fit formula and the $\Delta\mathcal{L}$ is added in the data simulation. For a data point, the $\Delta m_W$ caused by $\Delta\mathcal{L}$ can be written as:

$$\Delta m_W = \frac{\partial m_W}{\partial \sigma_{WW}} \sigma \cdot \sigma_{\mathcal{L}}. \tag{9}$$

Figure 5 (a) shows the dependence of $\Delta m_W$ on the energy with a fixed $\sigma_{\mathcal{L}}$, where the blue dots are the simulation results and red curve is the result of Eq. 9. It can be seen that the simulation results are consistent with the Eq. 9, and the contribution from $\sigma_{\mathcal{L}}$ will has a minimal point according to the product of the $W$-pair cross section and the partial derivative of $W$ mass to the $W$-pair cross section. The dependence of $\Delta m_W$ on the $\sigma_{\mathcal{L}}$ at a single data point with fixed energy, is shown in Fig. 5 (b), we can see that the $\Delta m_W$ associated with the uncertainty of luminosity at a specific energy point, almost increases linearly along with the $\sigma_{\mathcal{L}}$.

When there are more than one data point, the contribution from $\sigma_{\mathcal{L}}$ among different data points cannot considered in a independent way, due to the correlations. There is a more sophisticated way to consider the correlated systematic uncertainties by updating the $\chi^2$ definition [17], which is defined as:

$$\chi^2 = \sum_i \frac{(N_{\text{fit}^i} - N^i_{\text{obs}})^2}{\delta_i^2} + \frac{(h-1)^2}{\delta_c^2}, \tag{10}$$

where $\delta_i^2$ is the total statistical and uncorrelated systematic uncertainties, h is a free parameters, and $\delta_c^2$ is the total relative correlated systematic uncertainty. By using this method, the contributions from the correlated uncertainties can be reduced.

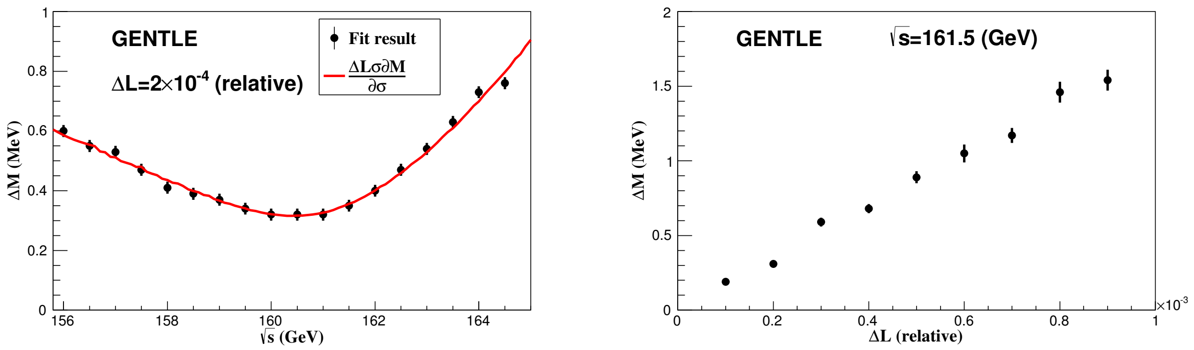


(a) (b)

Figure 5: (a)The distribution of the $\Delta m_W$ along with the energy, (b)the dependence of $\Delta m_W$ on the $\Delta\mathcal{L}$ at a specific energy point.

## 3 Data taking strategies

In the above section, we study the main sources of the uncertainties of $m_W$ ($\Delta\Gamma_W$ if there is more than one data point), including both the statistical and systematic ones. Generally, the $\Delta m_W$ ($\Delta\Gamma_W$) associated with these sources is depending on the energy of the data point, and the statistical part is also limited by the integrated luminosity of the data point. Based on the previous study, three data taking schemes are investigated, that are taking data at one, two, and three energy points.

In this paper, the following configurations are assumed for the different data taking schemes: the final uncertainty of the beam energy calibration is better than 0.5 MeV, $\Delta E < 0.5$ MeV; the beam energy spread can be well determined with its relative uncertainty less than 1%, $\Delta E_{BS} < 0.01$; and the total relative correlated systematic, $\delta^{\rm corr}_{\rm sys} \equiv \sqrt{\Delta\mathcal{L}^2 + \Delta\epsilon^2, +\Delta P^2 + \Delta\sigma^2_{\rm th}}$, less than $2 \times 10^{-4}$. The one standard derivation of $\Gamma_W$ from PDG [15] is used as its uncertainty, which is 42 MeV.

### 3.1 Measurement of $W$ mass at one energy point

For taking data at a single data point, there is a ideal strategy to measure the $m_W$ at the statistical sensitivity energy point, $E = 2m_W + 0.4 \approx 161.2$ GeV, which is shown in the Fig. 2 (a). But the contribution from systematic should be considered, especially for the added source, $\Gamma_W$. Figure 6 shows the distribution of $W$-pair cross section with the $W$ mass and width set at the PDG [15] average values $m_W = 80.385$ GeV, and $\Gamma_W = 2.085$ GeV, and with large 1GeV variation bands of the mass and width central values. We can seen that although the variation of the $W$ width changes the cross section lineshape, all the lineshapes of the cross sections with different $\Gamma_W$ will intersect at a energy point, $E = 2m_W + 1.5 \approx 162.3$ GeV, where the cross section is insensitive to the $W$ width.

Based on the study of the uncertainties of $m_W$, we try to take data at the two specific energy points individually. One is around the most statistical sensitive point, $E = 161.2$ GeV, and other one is $E = 162.3$ GeV, where there are very small contributions from the uncertainties of $\Gamma_W$ and the $E_{BS}$. Table 1 summarizes the results for taking at the above two energy points individually, with the configurations described above. We can see that the dominant contribution to $\Delta m_W$ at the most statistic sensitive point is from the uncertainty of $\Gamma_W$, which is negligible when taking data at $E = 162.3$ GeV. So taking data at 162.3 GeV is a good strategy when just measuring the $m_W$, and the corresponding precision is about 0.9 MeV.

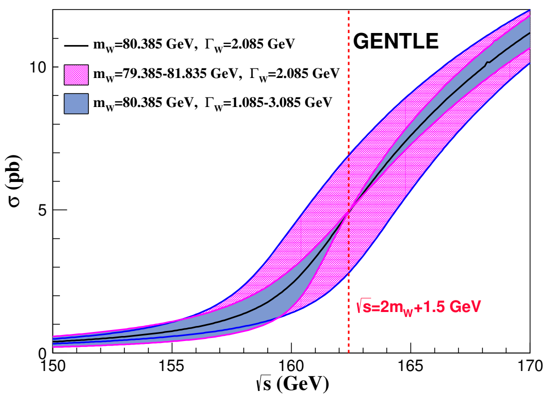


Figure 6: The distribution of $W$-pair cross section as a function the c.m. energy. The central curve corresponds to the result the PDG values of $m_W$ and $\Gamma_W$ [15]. Purple and green bands show the cross section curves obtained changing the $m_W$ and $\Gamma_W$ with 1 GeV.

Table 1: The precision of $m_W$ when taking data at $E = 161.2$ or 162.3 GeV. Shown in the table are the $\Delta m_W$ associated with the statistical uncertainty and the systematic uncertainties. The last column is the total $\Delta m_W$ at the corresponding energy point.

| Energy/source | | $\delta_{\rm stat}$ (stat.) | $\Delta E$ | $\Delta E_{BS}$ | $\Delta\Gamma_W$ | $\delta_{\rm sys}^{\rm corr}$ | Total |
|---|---|---|---|---|---|---|---|
| $\Delta m_W$ (MeV) | 161.2 (GeV) | 0.59 | 0.36 | 0.12 | 8.0 | 0.35 | 8.0 |
| | 162.3 (GeV) | 0.68 | 0.37 | - | - | 0.44 | 0.9 |

### 3.2 Measurement of $W$ mass and width at two energy points

When taking data at two different energy points near the $W$-pair threshold, the $m_W$ and $\Gamma_W$ can be measured simultaneously. In this situation, the uncertainties of the measured results, $\Delta m_W$ and $\Delta\Gamma_W$, cannot be obtained by the Eq. 5, due to the correlation between the two energy points. For each simulation, the statistical and uncorrelated systematic uncertainties, are assumed follow individual Poisson and Gaussian distributions for each energy point, respectively; and for each correlated systematic uncertainty, the same Gaussian distribution is used for all the energy points to consider the correlations. We repeat the simulation 500 times, the corresponding distributions of the $m_W$ and $\Gamma_W$ are follow the Gaussian distributions, with the means represent the nominal values and the one standard derivations includes contributions from both uncorrelated and correlated uncertainties.

To obtain the best measurements of $m_W$ and $\Gamma_W$ with the given assumptions, the energy points values, $E_1$ and $E_2$, as well as the luminosity fraction $F$ allocated to the lower energy point, should be optimized. So the 3-dimensional (3D) scan of the values of $E_1$, $E_2$, and $F$ is performed, with 100 MeV as the scan steps for energies and 0.05 for $F$.

The energy of most statistically sensitive point for $m_W$ is above $W$-pair threshold, but the one for $\Gamma_W$ is below the threshold, as shown is Fig. 2, which shows that the best precisions of $W$ mass and width cannot be reached with same energy point. So we define the object function to quantify the importance of them in the 3D scan, $T = m_W + A \cdot \Gamma_W$, where $A$ is a scale factor. Since $W$ mass is thought to be more important than its width, $A = 0.1$ is used throughout this paper, and the goal of 3D scan is turn to minimize the $\Delta T$ now. During the optimization of the scan parameter such as $E_1$, the different dependences of $\Delta T$ on $E_1$ are obtained by scanning other two parameters, than the value with minimum $\Delta T$ is taken as the optimized result for $E_1$.

Figure 7 (a)-(c) show the optimization of the $E_1$, $E_2$, and F, respectively. In practice, the 3D scan is performed, but the 2D plots are used to illustrate the optimization results for the scan parameters. When the dependence of $\Delta T$ on one parameter is plotted, another one is fixed with the scanning of the third one. For the minimal $\Delta T$, the three scan parameters are optimized as:

$$E_1 = 157.5\ \text{GeV}, \quad \text{E}_2 = 162.5\ \text{GeV}, \quad \text{F} = 0.3. \tag{11}$$

With these results, together with the configurations of total integrated luminosity and the control of the systematic uncertainties, the projected precisions for $m_W$ and $\Gamma_W$ are listed in Table 2.

### 3.3 Measurement of $W$ mass and width at three energy points

When taking data at three energy points near the $W$-pair threshold, the correlation between the different energy points can be taken into account during the $m_W$ and $\Gamma_W$ measurements by introducing a additional fit parameter $h$, as shown in Eq. 10. In this way, the dependence of the measurement(s) of $m_W$ ($\Gamma_W$) on the correlated systematic uncertainties, will be decreased, which means that the robustness of the measurements will be improved corresponding.

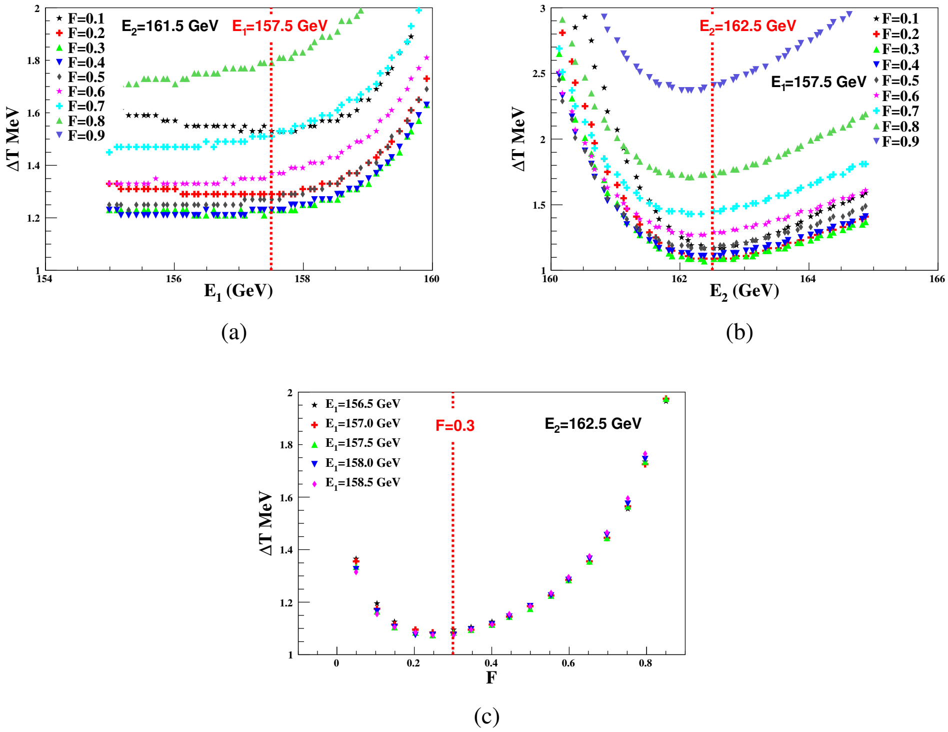


Figure 7: The optimization results of 3D scan for taking data at two points. (a)-(c) are for $E_1$, $E_2$, and $F$, respectively.

Table 2: The precision of $m_W$ and $\Gamma_W$ with the optimization result of taking data at two energy points, Shown in the table are the $\Delta m_W$ associated with the statistical uncertainty and the systematic uncertainties. The last column is the total projected uncertainties of $W$ mass and width.

| Source | $\delta_{\text{stat}}$ (stat.) | $\Delta E$ | $\Delta E_{BS}$ | $\delta_{\text{sys}}^{\text{corr}}$ | Total |
|---|---|---|---|---|---|
| $\Delta m_W$ (MeV) | 0.81 | 0.38 | - | 0.48 | 1.02 |
| $\Delta\Gamma_W$ (MeV) | 1.06 | 0.54 | 0.88 | 0.22 | 2.90 |

Based on the procedure of taking data at two energy points, the situation for three energy points becomes simple. The energies of the three data points, $E_1$, $E_2$, and $E_3$, as well as the two luminosity fractions $F_1$ and $F_2$, are optimized to obtain the best measurements of $m_W$ and $\Gamma_W$, where $F_1 = \mathcal{L}_1/\mathcal{L}$ and $F_2 = \mathcal{L}_2/(1-F_1)\mathcal{L}$. The scan procedure is similar as the one used for two energy points, but now the 3D scan is turn to be 5-dimensional (5D) scan, with additional 2 scan parameters. Figure 8 shows the optimization results for the 5D scan parameters, and for the minimal $\Delta T$, the three scan parameters are optimized as:

$$E_1 = 157.5\ \text{GeV},\ \mathrm{E}_2 = 162.5\ \text{GeV},\ \mathrm{E}_3 = 161.5\ \text{GeV},\ \mathrm{F}_1 = 0.3,\ \mathrm{F}_2 = 0.9. \tag{12}$$

With these results, together with the configurations of the total integrated luminosity and the control on the systematic uncertainties, the projected uncertainties would be

$$\Delta m_W \sim 1.0\ \text{MeV}, \quad \Delta\Gamma_{\mathrm{W}} \sim 2.8\ \text{MeV}. \tag{13}$$

The precisions of the $W$ mass and width with three energy points, is not improved much when compared with the results with two energy points. But the results with three energy points will be most stable, since the requirements of them on the correlated systematic uncertainties are broaden.

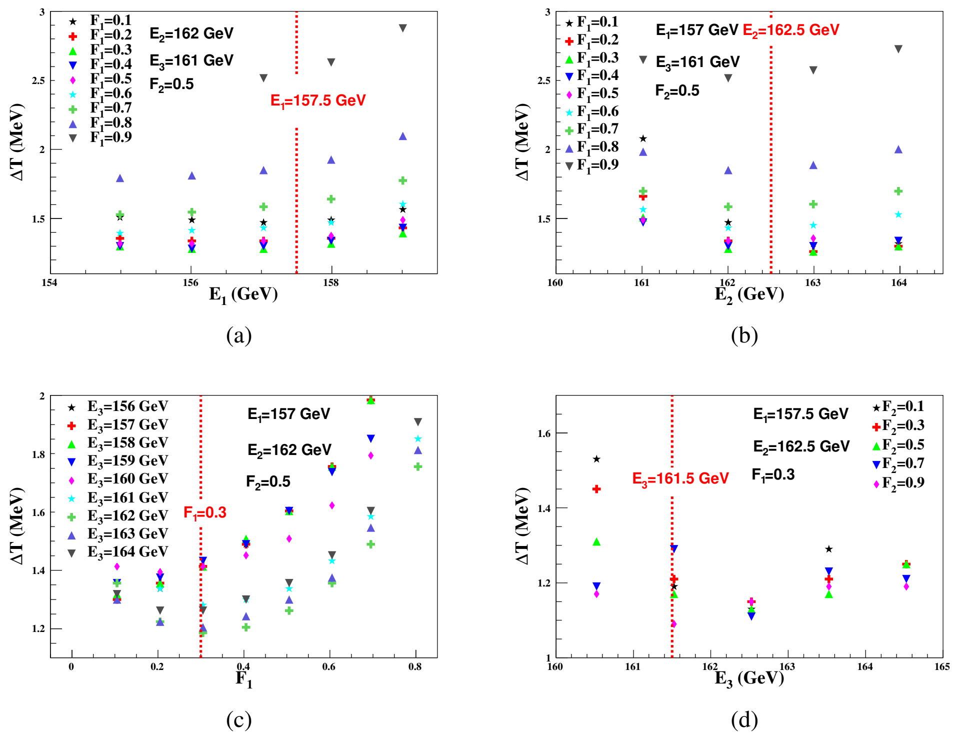


Figure 8: The optimization results of 5D scan for taking data at three points. (a)-(d) are the results for $E_1, E_2, F_1$, and $E_3$, respectively. The $F_2$ is also be optimized, which can be seen from (d).

### 3.4 Discussion about the data taking plan

In this section, three data taking schemes are investigated, based on different physical goal. With a given statistics of data and configurations of experiment (the controls of systematic uncertainties), the optimization of data taking is to minimize the total uncertainty, which is to find the balance between statistical and systematic uncertainties.

When the detector performance is excellent, as well as the high precision of the $W$-pair cross section calculation, the dominant limitation to the precision of $m_W$ and $\Gamma_W$ is statistical. Then taking data at few energy points will benefit to the final results, especially when we just measure the $m_W$, one energy point, around the region where $W$-pair cross section insensitive to $\Gamma_W$, is enough.

When the statistics of data is big enough, the dominant uncertainties of $m_W$ and $\Gamma_W$ are systematic. In this case, the well consideration of the systematic uncertainties is more important. The correlation between different energy points should be taken into account, especially for the uncertainties associated with the luminosity, the detection efficiency, the background contribution, and the calculation of the $W$-pair cross section. Based on this consideration, the number of data taking points is determined large than the number of measurements.

In this study, the optimized $\Delta m_W$ corresponding to three data points is just a litter bigger than the one with a single data point, but the $\Gamma_W$ could be measured simultaneously. So we think it is better to take data at three different data points, the corresponding parameters for these data points are optimized as Eq. 12.

# 4 Summary

In this paper, different data taking schemes are investigated to measure the $W$ boson mass at CEPC, based on the study of statistical and systematic uncertainties. With the given total integrated luminosity, $\mathcal{L} = 3.2\ \text{ab}^{-1}$, and the corresponding controls on the systematic uncertainties, the number of data points is determined as three, with the energies and luminosity allocations listed in Eq. 12. The corresponding projected total uncertainties of $W$ mass and width would be $\Delta m_W \sim 1.0$ MeV and $\Delta\Gamma_W \sim 2.8$ MeV, respectively.

## References


[1] S. L. Glashow, Nucl. Phys. **22** (1961) 579–588.

[2] A. Salam and J. C. Ward, Phys. Lett. **13** (1964) 168–171.

[3] S. Weinberg, Phys. Rev. Lett. **19** (1967) 1264–1266.

[4] F. Englert and R. Brout, Phys. Rev. Lett. **13** (1964) 321–323. [,157(1964)].

[5] P. W. Higgs, Phys. Rev. Lett. **13** (1964) 508–509. [,160(1964)].

[6] P. W. Higgs, Phys. Lett. **12** (1964) 132–133.

[7] UA1 Collaboration, G. Arnison et al., Phys. Lett. **B122** (1983) 103–116. [,611(1983)].

[8] UA1 Collaboration, G. Arnison et al., Phys. Lett. **B126** (1983) 398–410. [,7.55(1983)].

[9] UA2 Collaboration, M. Banner et al., Phys. Lett. **B122** (1983) 476–485. [,7.45(1983)].

[10] UA2 Collaboration, P. Bagnaia et al., Phys. Lett. **B129** (1983) 130–140. [,7.69(1983)].

[11] ATLAS Collaboration, G. Aad et al., Phys. Lett. **B716** (2012) 1–29, `arXiv:1207.7214 [hep-ex]`.

[12] CMS Collaboration, S. Chatrchyan et al., Phys. Lett. **B716** (2012) 30–61, `arXiv:1207.7235 [hep-ex]`.

[13] Gfitter Group Collaboration, M. Baak, J. Cth, J. Haller, A. Hoecker, R. Kogler, K. Mnig, M. Schott, and J. Stelzer, Eur. Phys. J. **C74** (2014) 3046, `arXiv:1407.3792 [hep-ph]`.

[14] J. de Blas, M. Ciuchini, E. Franco, S. Mishima, M. Pierini, L. Reina, and L. Silvestrini, JHEP **12** (2016) 135, `arXiv:1608.01509 [hep-ph]`.

[15] Particle Data Group Collaboration, C. Patrignani et al., Chin. Phys. **C40** no. 10, (2016) 100001.

[16] D. Yu. Bardin, J. Biebel, D. Lehner, A. Leike, A. Olchevski, and T. Riemann, Comput. Phys. Commun. **104** (1997) 161–187, `arXiv:hep-ph/9612409 [hep-ph]`.

[17] X.-H. Mo, HEPNP **31** (2007) 745–749.